



UNIVERSITY OF LEEDS

This is a repository copy of *Seismic response of Cfs strap-braced stud walls: Experimental investigation*.

White Rose Research Online URL for this paper:
<http://eprints.whiterose.ac.uk/99242/>

Version: Accepted Version

Article:

Iuorio, O, Macillo, V, Terracciano, MT et al. (3 more authors) (2014) Seismic response of Cfs strap-braced stud walls: Experimental investigation. *Thin-Walled Structures*, 85. pp. 466-480. ISSN 0263-8231

<https://doi.org/10.1016/j.tws.2014.09.008>

© 2014, Elsevier. Licensed under the Creative Commons Attribution-NonCommercial-NoDerivatives 4.0 International
<http://creativecommons.org/licenses/by-nc-nd/4.0/>

Reuse

Unless indicated otherwise, fulltext items are protected by copyright with all rights reserved. The copyright exception in section 29 of the Copyright, Designs and Patents Act 1988 allows the making of a single copy solely for the purpose of non-commercial research or private study within the limits of fair dealing. The publisher or other rights-holder may allow further reproduction and re-use of this version - refer to the White Rose Research Online record for this item. Where records identify the publisher as the copyright holder, users can verify any specific terms of use on the publisher's website.

Takedown

If you consider content in White Rose Research Online to be in breach of UK law, please notify us by emailing eprints@whiterose.ac.uk including the URL of the record and the reason for the withdrawal request.



eprints@whiterose.ac.uk
<https://eprints.whiterose.ac.uk/>

SEISMIC RESPONSE OF CFS STRAP-BRACED STUD WALLS: EXPERIMENTAL INVESTIGATION

Ornella IUORIO

*Department of Structures for Engineering and Architecture, University of Naples "Federico II",
Naples, Italy, ornella.iuorio@unina.it*

Vincenzo MACILLO

*Department of Structures for Engineering and Architecture, University of Naples "Federico II",
Naples, Italy, vincenzo.macillo@unina.it*

Maria Teresa TERRACCIANO

*Department of Structures for Engineering and Architecture, University of Naples "Federico II",
Naples, Italy, mariateresa.terracciano@unina.it*

Tatiana PALI

*Department of Structures for Engineering and Architecture, University of Naples "Federico II",
Naples, Italy, tatiana.pali@unina.it*

Luigi FIORINO

*Department of Structures for Engineering and Architecture, University of Naples "Federico II",
Naples, Italy, lfiorino@unina.it*

Raffaele LANDOLFO*

*Department of Structures for Engineering and Architecture, University of Naples "Federico II",
Naples, Italy, landolfo@unina.it*

***Corresponding Author:** Department of Structures for Engineering and Architecture, University of Naples "Federico II", Via Forno Vecchio 36, 80134 Naples ITALY; Phone: +39 081 2538052; Fax: +39 081 2538989

Keywords: Behaviour factor, Capacity design, Cold-formed steel, Wall tests, Seismic behaviour, Strap-braced stud walls.

HIGHLIGHTS

- The seismic behaviour of CFS strap-braced walls is evaluated by experimental investigation.
- The global inelastic response of a wide range of X-braced walls is discussed.
- The local behaviour is investigated by tests on material and connection systems.
- The behaviour factor provided by AISI S213 are confirmed by the experimental tests.
- The capacity design rules of Eurocodes are also reliable for the CFS structures.

ABSTRACT

The development of light weight steel structures in seismic area as Italy requires the upgrading of National Codes. To this end, in the last years a theoretical and experimental study was undertaken at the University of Naples within the Italian research project RELUIS-DPC 2010-2013. The study focused on "all-steel design" solutions and investigated the seismic behaviour of strap-braced stud walls. Three typical wall configurations were defined according to both elastic and dissipative design criteria for three different seismic scenarios. The lateral in-plane inelastic behaviour of these systems was evaluated by twelve tests performed on full-scale Cold-formed strap-braced stud wall specimens with dimensions 2400 x 2700 m subjected to monotonic and reversed cyclic loading protocols. The experimental campaign was completed with seventeen tests on materials, eight shear tests on elementary steel connections and twenty-eight shear tests on strap-framing connection systems. This paper provides the main outcomes of the experimental investigation. Furthermore, the design prescriptions, with particular reference to the behaviour factor and the capacity design rules for these systems, have been proved on the basis of experimental results.

INTRODUCTION

The Cold-Formed Steel (CFS) structures are able to ensure a good structural response in seismic areas. In these structures, the lateral load bearing systems are CFS stud walls, that are generally realized with frames in CFS profiles braced by sheathing panels or light gauge steel straps installed in a X configuration. The seismic behaviour of CFS structures laterally braced by panels ("sheathing-braced" approach) was the object of several studies carried out at the University of Naples "Federico II" in the last years. In particular, different experimental investigations were conducted on full-scale substructure prototypes (global response) and connections (local response) [1, 2, 3, 4, 5, 6, 7, 8].

When X-braced configuration is adopted, the design is carried out according to "all-steel" approach and steel straps are generally used to obtain the diagonal elements. In particular, because of the steel straps slenderness, only those in tension are considered active. Therefore, the lateral load applied on a wall is adsorbed only by the diagonal in tension, which transmits a significant axial compression

force to the ends of the wall. For this reason, the design of members and connections located at wall corners is crucial, especially for the chord studs, tracks, strap connections, gusset plate and anchors. Guidelines for the seismic design of CFS structures are not provided by the European codes (EN 1998-1 [9]). Hence, as an attempt to provide a contribution to the introduction of these systems in the European codes, a theoretical and experimental study was carried out at University of Naples Federico II. The research program, developed within the Italian research project RELUIS-DPC 2010-2013, was articulated in two main phases. An experimental phase devoted to the evaluation of the local and global behaviour of CFS strap-braced stud walls by means of laboratory tests on walls, materials and connection systems, which is presented in this paper, and a theoretical phase mainly devoted to define seismic design criteria, which is illustrated in the companion paper [10]. In the following, the results of the experimental phase are presented and discussed. In addition, on the basis of the experimental results, the adopted design assumptions for the seismic design of strap braced CFS structures are validated.

1 TEST PROGRAM

In order to investigate a wide range of possible CFS solutions for low-rise dwellings, three buildings to be located in different seismic area were designed. Each of them has a rectangular plan with dimensions 12.2 m x 18.1 m and storey height of 3.00 m. The lateral resisting system is made of CFS strap-braced stud walls that were designed according to elastic or dissipative design approaches. Therefore, three wall configurations were defined as follows: elastic light (WLE), dissipative light (WLD) and dissipative heavy (WHD) walls (Fig. 1). Table 1 shows the criteria adopted for the design of the diagonal straps, the non dissipative elements and the connections for the three different wall configurations. More details about the development of the case study and the design of walls are presented in the companion paper [10].

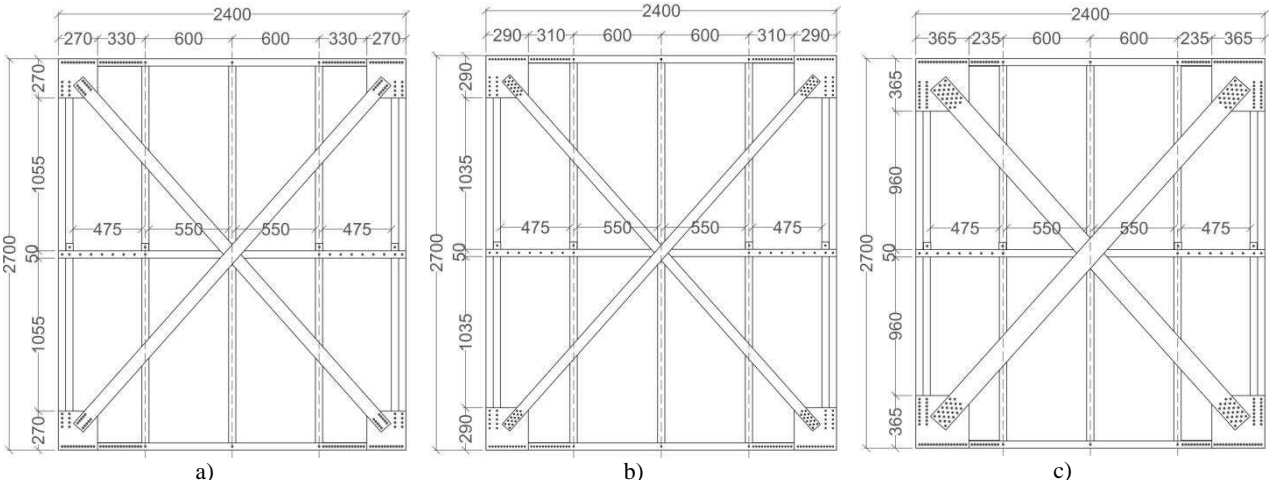


Figure 1. Schematic drawings of the three wall configurations: a) elastic light wall (WLE); b) dissipative light wall (WLD); c) dissipative heavy wall (WHD).

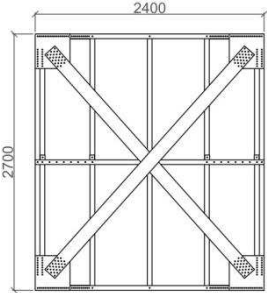
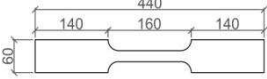
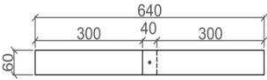
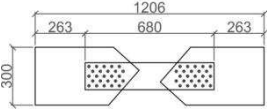
The lateral response of these systems was investigated by testing each of the three selected configurations by two monotonic and two cyclic tests for a total of twelve tests on full-scale wall specimens in size of 2400 x 2700 mm. Moreover, taking into account that materials and components influence the wall seismic global response in terms of lateral resistance, stiffness and ductility, the components response was investigated by means of seventeen tests on materials, eight shear tests on elementary screwed connections between steel profiles and twenty-eight shear tests on screwed connections between gussets and strap-bracings. The experimental campaign is summarized in Table 2. All tests were carried out in the laboratory of the Department of Structures for Engineering and Architecture of the University of Naples Federico II.

Table 1. Adopted design criteria.

Wall configuration		WLE	WLD	WHD
Net section fracture prevention	Eq (1): $N_{pl,Rd} \leq N_{u,Rd}$	NO	YES	YES
Forces for non dissipative elements	Eq (2): $R_d \geq 1.1 \cdot \gamma_{ov} \cdot R_{fy}$	NO	YES	YES
Brittle failure of fasteners	Eq (3): $F_{v,Rd} \geq 1.2F_{b,Rd}$ or $\Sigma F_{v,Rd} \geq 1.2F_{n,Rd}$	YES	YES	YES

$N_{pl,Rd}$: design plastic resistance of the diagonal cross section
 $N_{u,Rd}$: ultimate design resistance of the net cross section at fasteners holes
 R_d : connection resistance
 R_{fy} : design plastic resistance of the connected dissipative member
 $\gamma_{ov} = 1.25$: material overstrength factor
 $F_{v,Rd}$: shear resistance of the screw
 $F_{b,Rd}$: bearing resistance of the connection
 $F_{n,Rd}$: net area resistance of the connected member
 More details about Equations (1), (2) and (3) are given in the companion paper [10]

Table 2. Test matrix.

		WALLS			
		label	WLE	WLD	WHD
	no. monotonic tests		2	2	2
	no. cyclic tests		2	2	2
		MATERIALS			
		label	S350 - 1.5	S235 - 2.0	S350 - 3.0
	(steel grade - thickness in mm)				
	no. tests		3 _a + 3 _b	2 _a + 3 _b	3 _a + 3 _b
		ELEMENTARY CONNECTIONS			
		label	SLE	SLD	SHD
	no. tests		3 _b	3 _b	2 _b
		JOINTS between GUSSETS and STRAP-BRACINGS			
		label	CLE	CLD	CHD
	configuration		1	1 2 3 4	1 2 3 4
	no. tests		3 _a + 3 _b	3 _a + 3 _b 2 _b 2 _b 2 _b	1 _a + 3 _b 2 _b 2 _b 2 _b

_a stands for test speed equal to 50 mm/s;

_b stands for test speed equal to 0.05 mm/s;

WLE is Elastic Light Wall;

WLD is Dissipative Light Wall;

WHD is Dissipative Heavy Wall;

SLE is Single connection for Elastic Light wall;
SLD is Single connection for Dissipative Light wall;
SHD is Single connection for Dissipative Heavy wall;
CLE is Connection joint for Elastic Light wall;
CLD is Connection joint for Dissipative Light wall;
CHD is Connection joint for Dissipative Heavy wall

2 TESTS ON FULL-SCALE CFS STRAP-BRACED STUD WALLS

The lateral in-plane behaviour of the selected wall configurations (WLE, WLD, WHD) was investigated by means of twelve physical tests, including six monotonic tests and six cyclic tests on full-scale 2400 mm long and 2700 mm high wall specimens. The wall framing (Fig. 2a) was made with stud members, having lipped channel sections (C-sections), spaced at 600 mm on the center and connected at the ends to track members, having unlipped channel sections (U-sections). Since chord studs are subjected to higher axial load, aiming to avoid any buckling and failure of those studs, they were composed by double C-sections screwed back-to-back. In order to reduce the unbraced length of the chord and interior studs, flat straps were placed at the mid-height of the wall specimens and were screwed to blocking members placed at the ends of walls. The local buckling phenomena of tracks were avoided by reinforcing the ends of members with C-section profiles assembled in a box sections (Fig. 2b). Hold-down devices were placed within the lower and upper tracks at the four corners of the walls. They were made with steel grade S700 (characteristic yield strength $f_y = 700$ MPa and characteristic ultimate strength $f_u = 750$ MPa) and were connected to the studs by four M16 class 8.8 bolts and to the beams of the testing frame by one M24 class 8.8 bolt. The hold-downs transfer the uplift forces from the chord studs to the testing frame. The upper and bottom tracks of the tested walls were connected respectively to the loading (top) and bottom beams of the testing frame by M8 class 8.8 bolts spaced at 300 mm on the center, which were used as shear connections. The wall specimens were completed with strap braces installed in an X configuration on both sides and connected to the wall framing by gusset plates. For each wall configuration an appropriate fastener was chosen: 6.3 x 40 mm (diameter x length) hexagonal flat washer head self-drilling screws (AB 04 63 040 type) for WLE and WHD specimens, and 4.8 x 16 mm modified truss head self-drilling screws (CI 01 48 016 type) for WLD prototypes, produced by Tecfi S.p.A. [11]. All the steel members were fabricated by steel grade S350GD+Z ($f_y = 350$ MPa and $f_u = 420$ MPa), except the diagonal straps of dissipative systems, which were made with steel grade S235 ($f_y = 235$ MPa and $f_u = 360$ MPa). Table 3 lists the nominal design dimensions and material properties of the tested wall components and Table 4 summarizes the adopted connection systems. Schematic drawings of the WHD configuration is provided in Figure 2 and photos of the three wall configurations with the corresponding corner details are provided in Figure 3 through Figure 5.

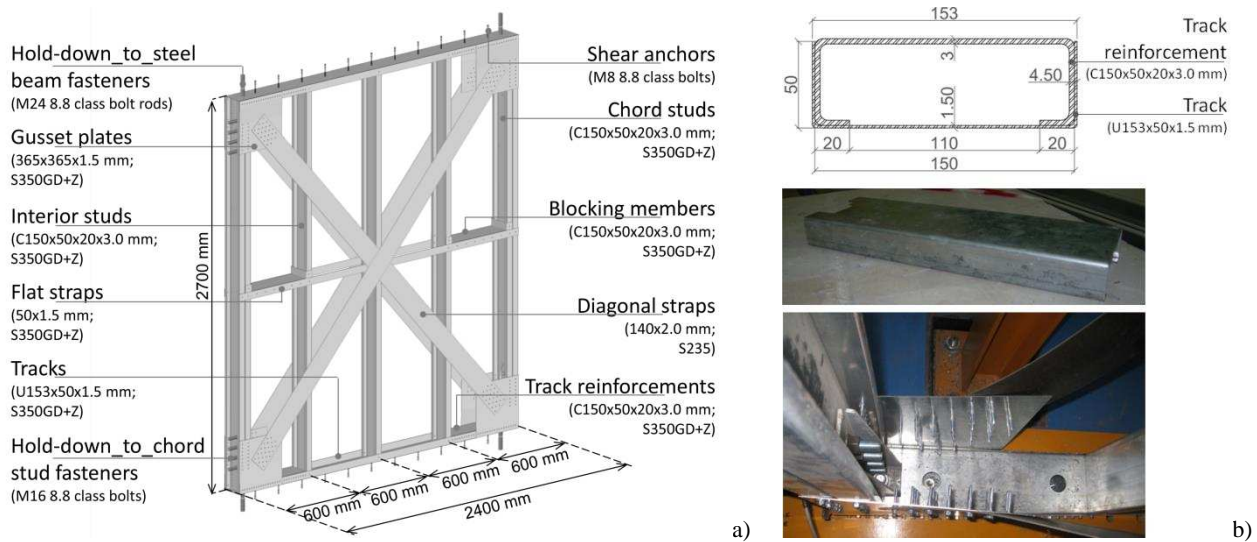


Figure 2. WHD wall configuration: a) indication of the wall components and their dimensions; b) track reinforcement detail.

Table 3. Nominal design dimensions and material properties of the tested wall components.

	WLE		WLD		WHD	
	Section [mm]	Grade	Section [mm]	Grade	Section [mm]	Grade
Studs	C150x50x20x1.5 ^a	S350	C150x50x20x1.5 ^a	S350	C150x50x20x3.0 ^a	S350
Tracks	U153x50x1.5 ^b	S350	U153x50x1.5 ^b	S350	U153x50x1.5 ^b	S350
Diagonal straps	90x1.5 ^c	S350	70x2.0 ^c	S235	140x2.0 ^c	S235
Gusset plates	270x270x1.5 ^d	S350	290x290x1.5 ^d	S350	365x365x1.5 ^d	S350
Track reinforcements	C150x50x20x1.5 ^a	S350	C150x50x20x1.5 ^a	S350	C150x50x20x3.0 ^a	S350
Blocking members	C150x50x20x1.5 ^a	S350	C150x50x20x1.5 ^a	S350	C150x50x20x3.0 ^a	S350
Flat straps	50x1.5 ^c	S350	50x1.5 ^c	S350	50x1.5 ^c	S350

^a C-section: outside-to-outside web depth x outside-to-outside flange size x outside-to-outside lip size x thickness;
^b U-section: outside-to-outside web depth x outside-to-outside flange size x thickness;
^c width x thickness;
^d height x width x thickness

Table 4. Adopted connection systems.

	WLE	WLD	WHD
Screws	AB 04 63 040	CI 01 48 016	AB 04 63 040
Shear anchors	M8 class 8.8 bolts spaced at 300 mm on centre		
Hold-down_to_chord stud fasteners	no.4 M16 class 8.8 bolts		
Hold-down_to_steel beam fasteners	M24 class 8.8 bolt rods		



Figure 3. WLE_M1 general view and corner detail.



Figure 4. WLD_M2 general view and corner detail.

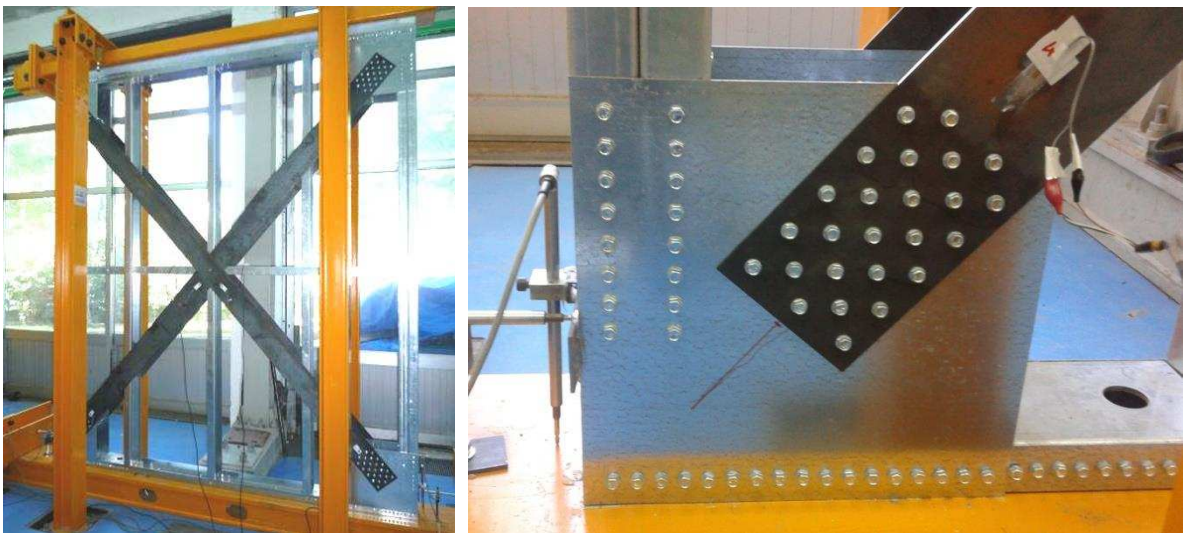


Figure 5. WHD_M1 general view and corner detail.

Tests on full-scale wall specimens were carried out by using a specifically designed testing frame for in-plane shear loading (Fig. 6). Horizontal loads were transmitted to the upper wall track by means of a steel beam made of a 200x120x10 mm (width x height x thickness) rectangular hollow section.

The wall prototype was constrained to the laboratory strong floor by the bottom beam of testing frame. The horizontal component of the brace force was transfer through the track to the supporting structure. The out-of-plane displacements of the wall were avoided by two lateral supports realized with HEB 140 columns and equipped with double roller wheels. The tests were performed by using a hydraulic actuator having ± 250 mm stroke displacement and 500 kN load capacity. A sliding-hinge was placed between the actuator and the tested wall in order to avoid the transmission of external vertical load components. Eight LVDTs were used to measure the specimen displacements. In particular, three LVDTs (W_1 , W_2 e W_3) were installed to record the horizontal displacements (W_1 for the top displacements, W_2 and W_3 for the displacements at the bottom of the walls) and two LVDTs (W_4 , W_5) for the vertical displacements. The local deformations of the diagonal straps were recorded by means of two strain-gauges for each diagonal (S_1 and S_4 placed at the end and S_2 and S_3 placed in the center of the straps). A load cell was used to measure the applied loads.

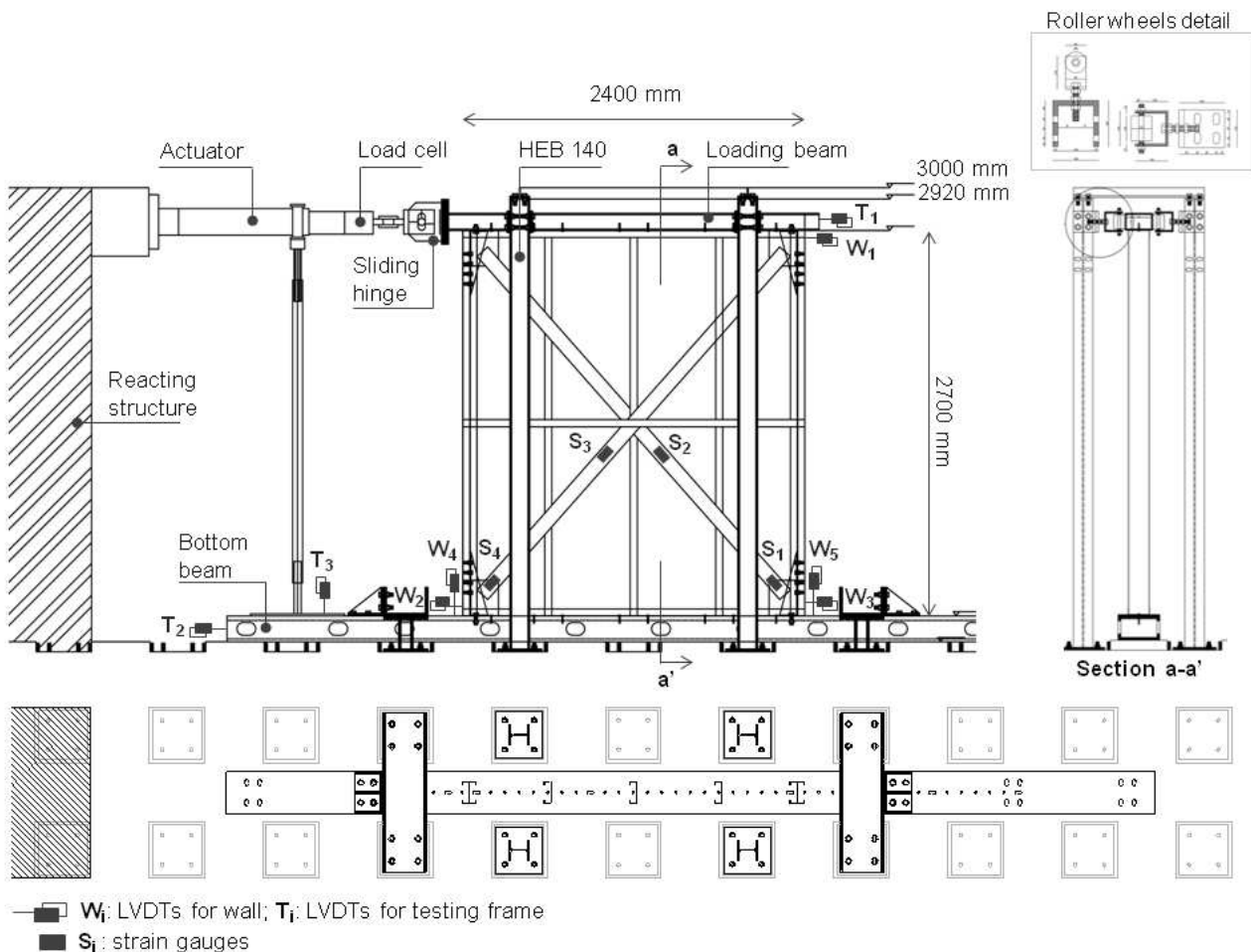


Figure 6. Test on full-scale walls.

2.1 Monotonic tests

In the monotonic loading regime, the tests were performed by applying a loading protocol organized in two phases. In the first phase the wall specimens were pulled and in the second phase they were

pushed. Both phases have been followed by the unloading of the wall prototypes in order to lead them back to the initial position. Figure 7 shows the response curve in terms of load vs. displacement for WLE-M2 specimen. This testing protocol involved displacements at a rate of 0.10 mm/s up to a maximum of ± 240 mm defined by the stroke limit of the actuator or until the occurred collapse.

Test results in terms of yield strength (H_y), maximum strength (H_{max}), displacement at the conventional elastic limit (d_y), maximum displacement (d_{max}), conventional elastic stiffness (k_e), defined as the secant stiffness at 40% of the maximum strength, and observed failure mechanisms are shown in Table 5. In addition, Table 5 provides the theoretical predicted values of the wall strength and stiffness together with the ratios between the average experimental and theoretical values. The latter were evaluated according to the EN 1993-1-3 [12] through the methodology illustrated in Sections 3 of the companion paper [10] by using the average experimental mechanical properties. Figure 8 through Figure 10 show the acting load (H) vs top wall displacement (d) curves for the WLE-M1, WLD-M1 and WHD-M2 prototypes with the experimental values measured in the pulling and pushing phases (indicated with subscripts - and +, respectively) and the predicted parameters (indicated with subscript p), which are used to evaluate the structural response. Moreover, the interstorey-drift levels, which are defined as the ratio (d/h) between the top wall displacement and wall height set equal to 2700 mm, are also provided in the wall specimen curves.

Test results reveal a decrement of maximum strength contained within 12% in the pushing phase with respect to the pulling phase, while the conventional elastic stiffness records significant decrement up to 42% in the pushing phase, due to the occurrence of local damages of some wall components in the previous pulling phase. Moreover, the strength prediction is very close to the experimental results, with a maximum difference of 9% of the average experimental values compared to the theoretical strength values. In addition, the ratios between the average experimental and theoretical stiffness demonstrate that the experimental values are lower than the theoretical predictions, with variations ranging between 8% and 47%.

In agreement with the predicted failure mechanisms, the WLE configurations collapse was reached with the net section failure of diagonal straps (Fig. 11a), while the performance of WLD and WHD specimens was governed by the brace yielding up to the maximum stroke of the actuator without reaching the wall failure (Fig. 11b, Fig. 11c and Fig. 11d). The dissipative walls were displaced to significantly higher drift levels (in the range of 5.1% through 9.0% for WLD walls and in the range of 5.8% through 8.1% for WHD specimens) compared with elastic walls (in the range of 1.0% through 1.4%).

Regarding the dissipative heavy wall, in the first test (WHD-M1) a temporary strength loss was recorded (Fig. 12a), which was due to the occurrence of local buckling at the non-reinforced fields of the track for effect of high compression loads (Fig. 12b). In order to prevent this phenomenon, in the

second test (WHD-M2) the track reinforcement was extended to the full tracks (Fig. 12c) and the experimental response demonstrated the effectiveness of the intervention (Fig. 12a).

The wall stiffness can be evaluated by taking into account the stiffness contributions due to main wall structural components: (K_d) related to the axial deformability of the diagonals in tension, (K_c) due to the deformability of the diagonal-to-frame connections and (K_a) corresponding to the deformation of the anchors in tension. In particular, this last can be evaluated on the basis of the wall monotonic tests, as defined in [10]. Specifically, the stiffness (k_a) experimental value of the anchorage system in tension (chord stud bolts, hold-down device and rod) was defined as the ratio between the vertical force acting in the chord stud and the up-lift displacements registered at the bottom of the wall (W_5 LVDT) in the pulling phase (Fig. 13a). Figure 13b shows the curves in terms of the axial stiffness of the anchorage system in tension (k_a) vs the displacement (d) registered at the top of the wall. Taking into account that the recorded conventional elastic limit displacement (d_y) is in the range of about 15 and 30 mm, the axial stiffness for the tension anchors range in the range from 15 to 24 kN/mm, with an average value of about 20 kN/mm.

Table 5. Test results of monotonic tests on full-scale walls.

Label	H_y [kN]		H_{max} [kN]		d_y [mm]		d_{max} [mm]		k_c [kN/mm]		Failure mode	
	pull	push	pull	push	pull	push	pull	push	pull	push	pull	push
WLE-M1	64.9	65.6	66.3	66.6	18.5	24.3	36.7	35.3	3.5	2.7	NSF	NSF
WLE-M2	65.9	63.7	67.6	64.3	15.0	15.5	30.2	27.1	4.4	4.1	NSF	NSF
exp _{AV}	65.4	64.7	67.0	65.5	16.8	19.9	33.5	31.2	4.0	3.4	-	-
th	-	-	61.4	61.4	-	-	-	-	4.4	4.4	NSF	NSF
exp _{AV} / th	-	-	1.09	1.07	-	-	-	-	0.90	0.77	-	-
WLD-M1	56.7	58.8	61.7	62.3	14.2	18.4	214.5	244.2	4.0	3.2	BY	BY
WLD-M2	56.0	54.4	64.2	56.5	13.0	17.0	237.9	139.0	4.3	3.2	BY	BY
exp _{AV}	56.4	56.6	63.0	59.4	13.6	17.7	226.2	191.6	4.2	3.2	-	-
th	55.0	55.0	-	-	-	-	-	-	4.9	4.9	BY	BY
exp _{AV} / th	1.02	1.03	-	-	-	-	-	-	0.85	0.65	-	-
WHD-M1	110.3	107.8	116.9	119.3	17.8	29.9	157.6	159.7	6.2	3.6	BY	BY
WHD-M2	109.5	114.2	118.4	119.3	18.6	33.6	203.5	220.0	5.9	3.4	BY	BY
exp _{AV}	109.9	111.0	117.7	119.3	18.2	31.8	180.6	189.9	6.1	3.5	-	-
th	110.0	110.0	-	-	-	-	-	-	6.6	6.6	BY	BY
exp _{AV} / th	1.00	1.01	-	-	-	-	-	-	0.92	0.53	-	-

exp_{AV} : average experimental values;

th: theoretical values;

BY: brace yielding;

NSF: net section failure of strap-bracing

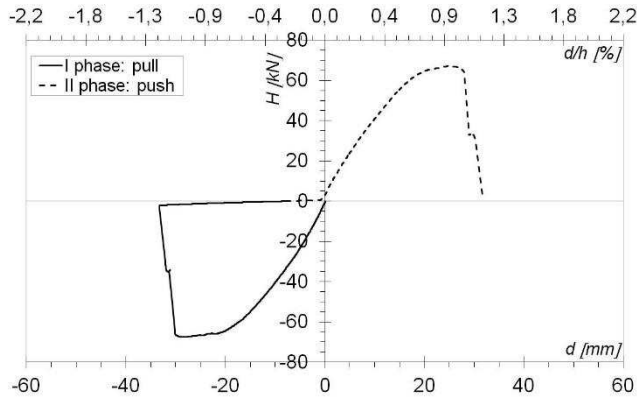


Figure 7. Response curve in terms of load vs. displacement for WLE-M2.

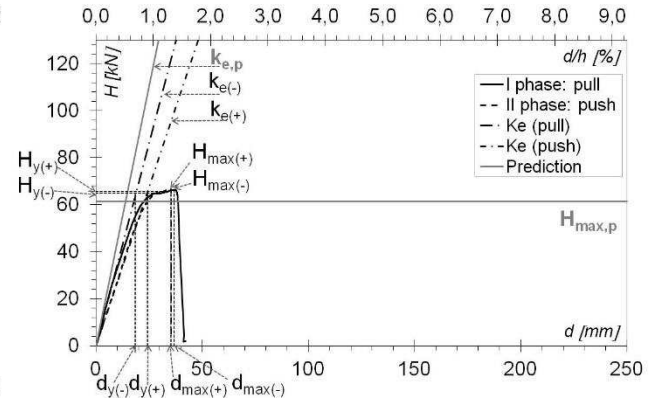


Figure 8. Monotonic test on WLE-M1 specimen: load vs. displacement curve.

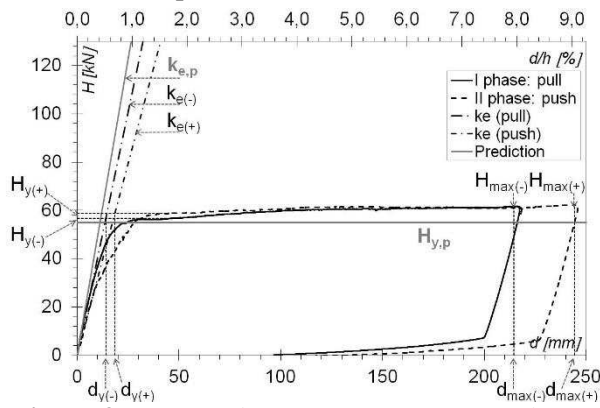


Figure 9. Monotonic test on WLD-M1 specimen: load vs. displacement curve.

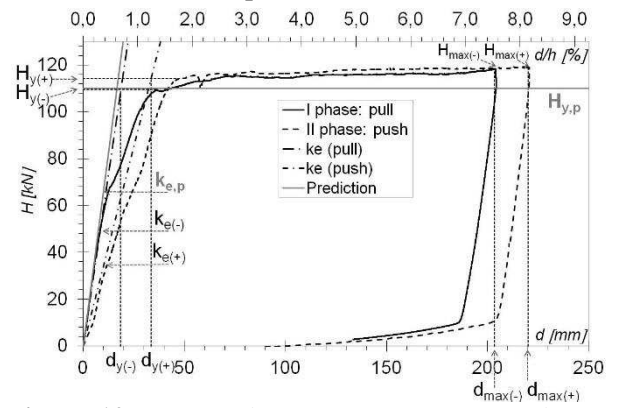


Figure 10. Monotonic test on WHD-M2 specimen: load vs. displacement curve.

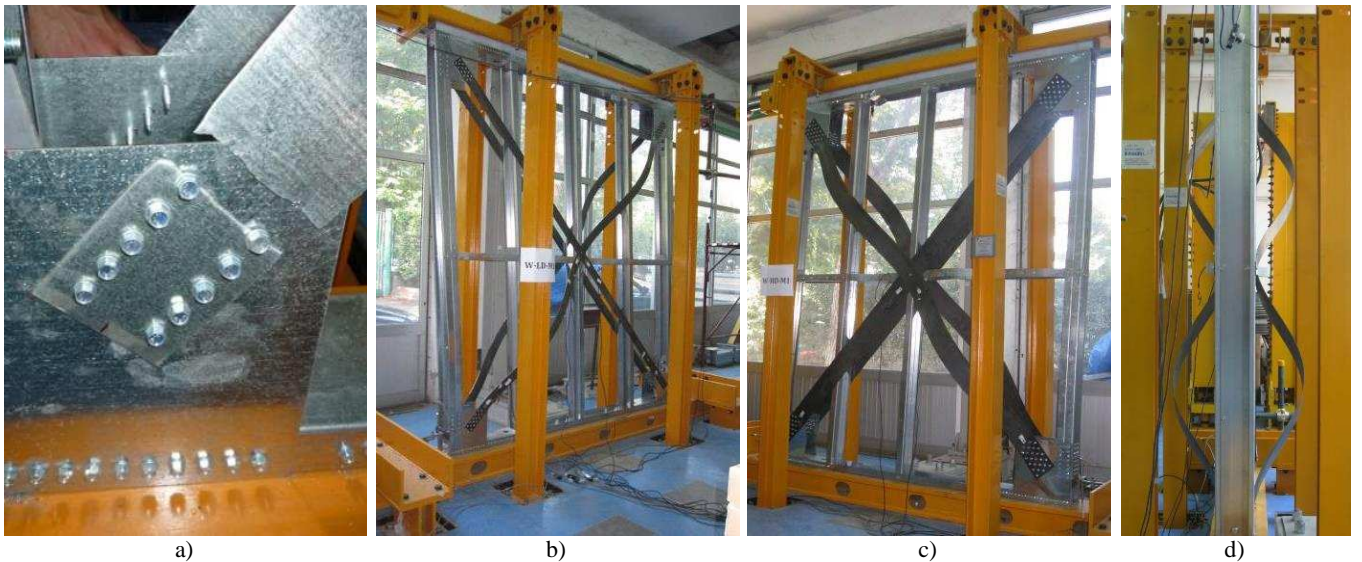
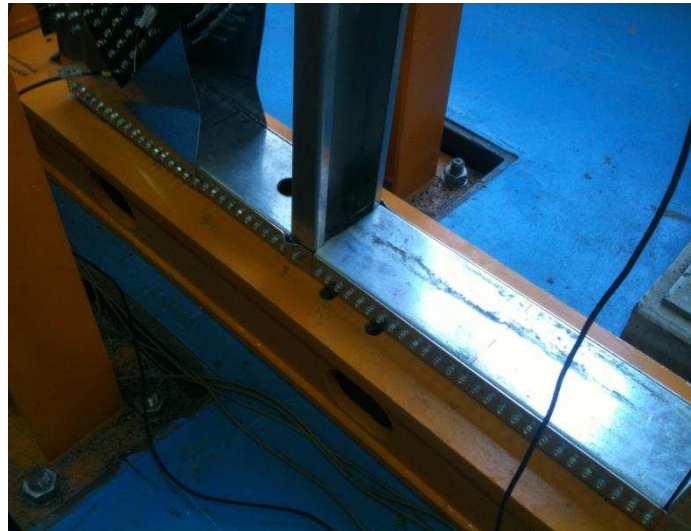
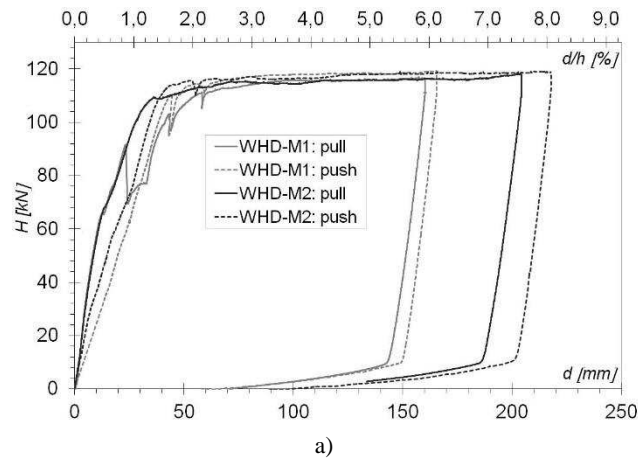


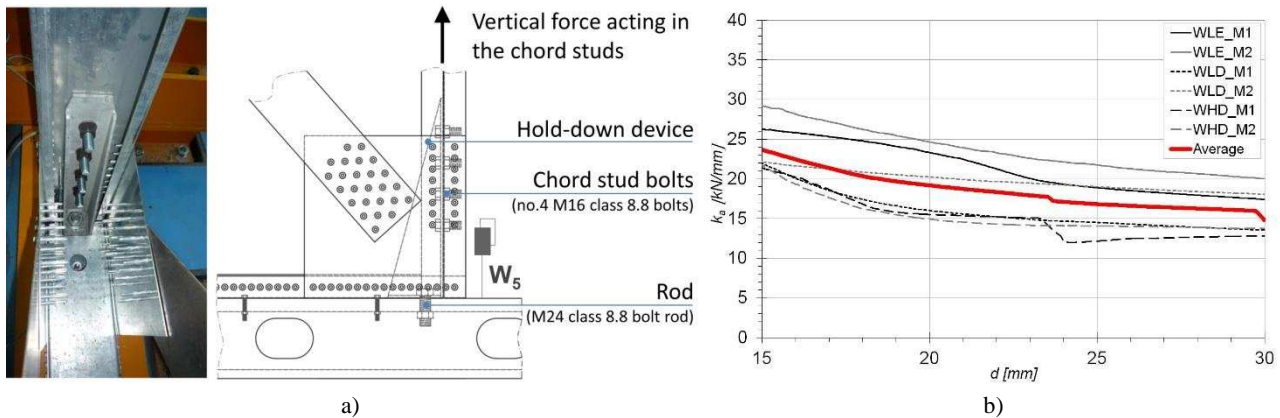
Figure 11. Collapse mechanism for the monotonic tests: a) net section failure for WLE-M1; b) brace yielding for WLD-M1; c) and d) brace yielding for WHD-M1.



b)

c)

Figure 12. Dissipative heavy walls: a) comparison between the response curve of WHD-M1 and WHD-M2; b) track reinforcement adopted in WHD-M1 and; c) track reinforcement adopted in WHD-M2.



a)

b)

Figure 13. Definition of the stiffness experimental value of the tension device: a) hold-down detail for WHD-M1; b) curve in terms of k_a vs. d .

2.2 Cyclic tests

The cyclic tests were carried out by adopting a loading protocol known as "CUREE ordinary ground motions reversed cyclic load protocol" developed for wood walls by Krawinkler et al. [14] and modified for CFS strap-braced stud walls by Velchev et al. [15]. The cyclic loading test protocol consists of a series of stepwise increasing deformation cycles. The displacement amplitudes were

defined starting from a reference deformation $\Delta = 2.667\Delta_y$, where Δ_y was defined as the displacement at the conventional elastic limit evaluated in the nominally identical monotonic wall tests. The cyclic protocol involved displacements at a rate of 0.5 mm/s, for displacements up to 9.97 mm, 7.36 mm e 7.27 mm for WLE, WLD and WHD walls respectively, and of 2.0 mm/s for displacement greater than those above mentioned. The adopted test protocol for WLE specimens is shown in Fig. 14.

The results of the cyclic tests are shown in Table 6, in which the theoretical values of the wall strength and stiffness are the same ones provided for the monotonic tests. Figure 15 through Figure 17 provide the acting load (H) versus the measured displacement (d) curves and the analyzed parameters for the WLE-C1, WLD-C2 and WHD-C1 specimens.

Table 6. Test results of cyclic tests on full-scale walls.

Label	H_y [kN]		H_{max} [kN]		d_{max} [mm]		k_e [kN/mm]		Failure mode	
	pull	push	pull	push	pull	push	pull	push	pull	Push
WLE-C1	69.6	68.9	70.6	69.4	38.1	35.7	3.7	3.4	NSF	NSF
WLE-C2	68.0	69.9	68.3	70.5	26.5	31.3	4.0	4.7	NSF	NSF
exp _{AV}	68.8	69.4	69.5	70.0	32.3	33.5	3.9	4.1	-	-
th	-	-	61.4	61.4	-	-	4.4	4.4	NSF	NSF
exp _{AV} / th	-	-	1.13	1.14	-	-	0.88	0.92	-	-
WLD-C1	58.7	59.8	63.1	64.4	176.2	165.5	3.8	4.0	NSF	NSF
WLD-C2	58.7	60.0	66.6	64.9	141.2	144.8	4.6	4.5	NSF	NSF
exp _{AV}	58.7	59.9	64.9	64.7	158.7	155.2	4.2	4.3	-	-
th	55.0	55.0	-	-	-	-	4.9	4.9	BY	BY
exp _{AV} / th	1.07	1.09	-	-	-	-	0.86	0.87	-	-
WHD-C1	116.7	116.0	124.0	124.2	197.0	221.0	5.7	7.7	NSF	BY
WHD-C2	112.9	111.6	118.9	124.2	67.5	221.8	7.5	6.7	NSF	BY
exp _{AV}	114.8	113.8	121.5	124.2	132.3	221.4	6.6	7.2	-	-
th	110.0	110.0	-	-	-	-	6.6	6.6	BY	BY
exp _{AV} / th	1.04	1.03	-	-	-	-	1.00	1.09	-	-

exp_{AV}: average experimental values;
th: theoretical values;
BY: brace yielding;
NSF: net section failure of strap-bracing

The results show that the strength and stiffness recorded in the pushing phase with respect to the pulling phases have maximum differences of 4% and 18%, respectively, except a variation of 35% for the stiffness of WHD-C1 specimen. The ratios between the average experimental and theoretical values highlight that the experimental strengths are higher than the theoretical predictions with maximum difference of 14%, while the measured stiffness values are lower than the predicted parameters with a variation up to 14%.

For all prototypes the observed collapse mode was the net section failure of diagonal straps (Fig. 18), except for WHD wall specimens, that showed the brace yielding in the pushing. As in the case of monotonic tests, the dissipative walls exhibited significantly higher drift levels (in the range of 5.2% through 6.5% for WLD walls and in the range of 2.5% through 8.2% for WHD specimens) compared with elastic walls (in the range of 1.0% through 1.4%).

The comparison between the monotonic and cyclic test results reveals that the average experimental shear strength and stiffness values registered under monotonic loads are lower than the one recorded in the cyclic tests with maximum variations of 8% and 16%, respectively, except the case of the WHD specimens affected by local damages in the monotonic tests.

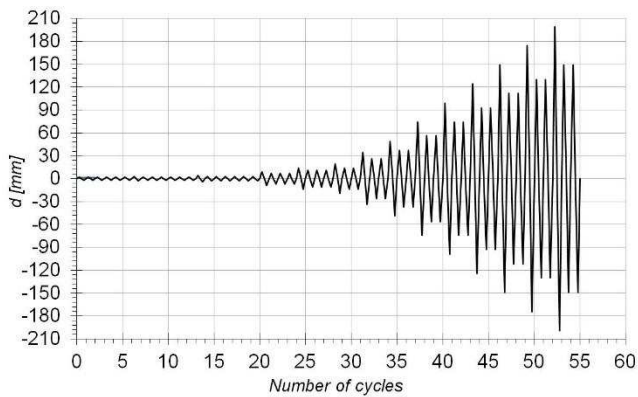


Figure 14. Cyclic protocol for WLE specimens.

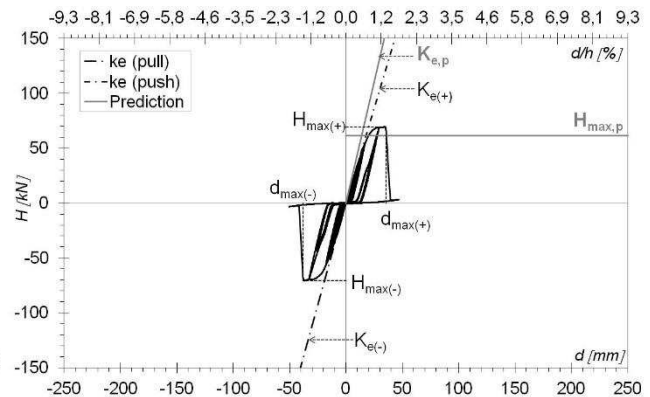


Figure 15. Cyclic test on WLE-C1 specimen: load vs. displacement curve.

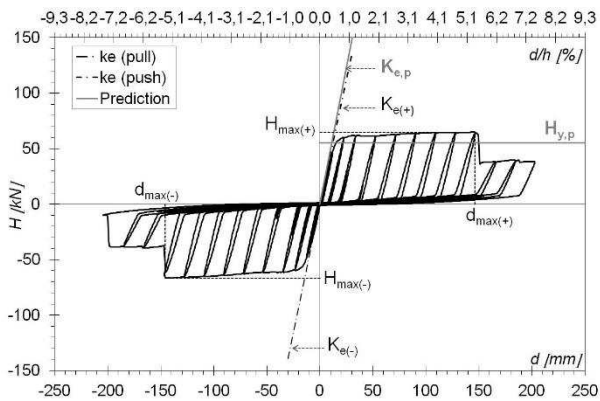


Figure 16. Cyclic test on WLD-C2 specimen: load vs. displacement curve.

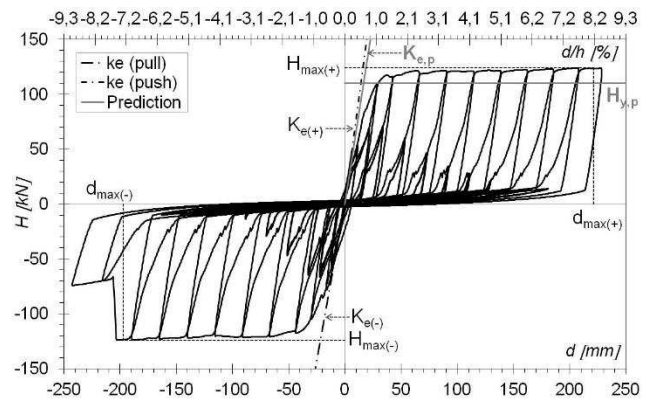


Figure 17. Cyclic test on WHD-C1 specimen: load vs. displacement curve.

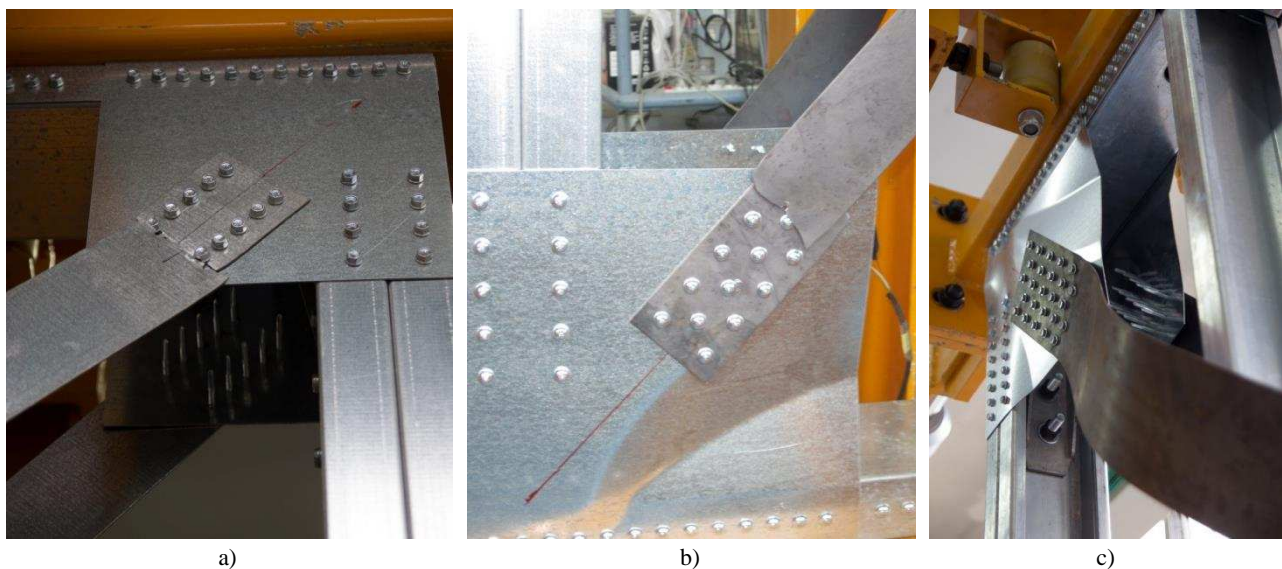


Figure 18. Net cross-section fracture for a) WLE-C2 and b) WLD-C2; c) strap yielding registered in WHD-C1.

3 TESTS ON MATERIAL AND COMPONENTS

3.1 Test on materials

The material coupons of straps and frame members were subjected to conventional tension tests according to EN ISO 6892-1 [16]. In particular, tests were performed on three specimen types S235-2.0, S350-1.5, S350-3.0, characterized by steel grades S235 with thickness of 2.0 mm and S350GD+Z with thicknesses of 1.5 mm and 3.0 mm (Table 7). Since the effects of "strain rate" were not assessed with the wall tests, in which the maximum displacement rate was 0.5 mm/s, therefore tests on material at standard rate (0.05 mm/s) and high rate (50 mm/s) were carried out for each specimen type. The high displacement rate corresponds to strain rate in the range from 0.10 to 0.15 s⁻¹. It was selected in such a way to obtain strain rates comparable with those used in wall cyclic tests with high rate displacements, i.e. wall tests carried out by Velchev and Rogers [17] and Serrette [18], in which maximum strain rates of about 0.08 and 0.12 s⁻¹ was nominally imposed at straps, respectively.

Table 7. Mechanical properties for tests on materials.

Specimen type	Steel grade	Thickness [mm]	$f_{y,n}$ [MPa]	$f_{u,n}$ [MPa]	$f_{u,n} / f_{y,n}$
S235-2.0	S235	2.0	235	360	1.5
S350-1.5	S350GD+Z	1.5	350	420	1.2
S350-3.0	S350GD+Z	3.0	350	420	1.2

$f_{y,n}$: nominal yield strength;
 $f_{u,n}$: nominal ultimate strength

Table 8. Tests results on materials.

Label	$f_{y,exp}$ [MPa]		$f_{u,exp}$ [MPa]		$f_{y,exp}/f_{y,n}$		$f_{u,exp}/f_{u,n}$		$f_{u,exp} / f_{y,exp}$		$f_{y,exp(H)} / f_{y,exp(S)}$	$f_{u,exp(H)} / f_{u,exp(S)}$
	S	H	S	H	S	H	S	H	S	H		
S235-2.0-01	311	335	381	403	1.32	1.43	1.06	1.12	1,23	1,20	1.08	1.06
S235-2.0-02	294	310	360	376	1.25	1.32	1.00	1.04	1,22	1,21	1.05	1.04
S235-2.0-03	300	-	358	-	1.28	-	0.99	-	1,19	-	-	-
Average values	302	323	366	390	1.28	1.37	1.02	1.08	1,21	1,21	1.07	1.05
S350-1.5-01	355	390	408	431	1.01	1.11	0.97	1.03	1,15	1,11	1.10	1.06
S350-1.5-02	359	374	412	431	1.03	1.07	0.98	1.03	1,15	1,15	1.04	1.05
S350-1.5-03	352	376	407	430	1.01	1.07	0.97	1.02	1,16	1,14	1.07	1.06
Average values	355	380	409	431	1.02	1.09	0.97	1.03	1,15	1,13	1.07	1.05
S350-3.0-01	368	389	430	453	1.05	1.11	1.02	1.08	1,17	1,16	1.06	1.05
S350-3.0-02	363	385	423	454	1.04	1.10	1.01	1.08	1,17	1,18	1.06	1.07
S350-3.0-03	361	388	423	455	1.03	1.11	1.01	1.08	1,17	1,17	1.07	1.08
Average values	364	387	425	454	1.04	1.11	1.01	1.08	1,17	1,17	1.06	1.07

$f_{y,exp}$: experimental yield strength;
 $f_{u,exp}$: experimental ultimate strength;
 $f_{y,n}$: nominal yield strength;
 $f_{u,n}$: nominal ultimate strength;
H: high rate (50 mm/s);
S: standard rate (0.05 mm/s);

Table 8 shows the experimental yield ($f_{y,exp}$) and ultimate strength ($f_{u,exp}$) for each test and the average values. In addition, Table 8 shows the ratio between experimental and nominal values of yield and ultimate strength for standard and high rates, the ratio between experimental ultimate and yield

strength and the ratio between experimental values of yield and ultimate strength obtained at high ($f_{y,exp(H)}$ and $f_{u,exp(H)}$) and standard ($f_{y,exp(S)}$ and $f_{u,exp(S)}$) rates.

As regard the tests at standard rate, the average experimental values of the yield strength are larger than the nominal values (28%, 2%, 4% for S235-2.0, S350-1.5, S350-3.0, respectively), while the results in terms of average experimental ultimate strength record a moderate increment for S235-2.0 and S350-3.0 specimens (2% e 1%, respectively) and a reduction of 3% for S350-1.5 specimens.

In order to achieve the gross cross-section yielding of the diagonal strap bracing member prior than the net section failure, the AISI S213 [19] provides an important requirement about the steel material property used for straps. This requirement can be expressed as the ratio between expected ultimate and yield strength, that should be greater than or equal to 1.2. The ratios between experimental ultimate and yield strength ($f_{u,exp} / f_{y,exp}$) obtained by material tests are provided for each test in Table 8.

Considering the S235 steel grade, which is that used for dissipative walls (walls designed in such a way that the design plastic resistance of the diagonal cross section is less than the ultimate design resistance of the net cross section at fasteners holes), the $f_{u,exp} / f_{y,exp}$ ratios ranged from 1.19 to 1.23, thus are very close to the limit imposed by AISI S213 (1.2). This circumstance increased the possibility of net section rupture in the braces.

The "strain-rate" effect produced an increment of the strength. In particular, the yield and ultimate strength increased between 5% and 7% as the test rate increased.

3.2 Test on elementary connections

In order to investigate the shear behaviour of the elementary connections between frame and strap-bracing, lap shear tests were carried out according to the procedure described in ECCS TC7 TWG 7.10 [20]. Three connection configurations, corresponding to each of the investigated wall typologies, were tested at standard rate (0.05 mm/s) (Table 9): (SLE) connections between 1.5 mm thick S350GD+Z steel plates with 6.3 mm diameter self-drilling screws; (SLD) connections between 1.5 mm thick S350GD+Z and 2.0 mm thick S235 steel plates with 4.8 mm diameter self-drilling screws; (SHD) connections between 1.5 mm thick S350GD+Z and 2.0 mm thick S235 steel plates with 6.3 mm diameter self-drilling screws. Table 10 lists the results in terms of failure load (F_t), stiffness (k_e) and failure mechanisms. Furthermore, Table 10 provides the average experimental values, standard deviation and coefficient of variation (C.O.V.) for strength and stiffness and the ratios between the average experimental and theoretical strength values, which are evaluated according to the EN 1993-1-3 [12] and using the average experimental mechanical properties.

Table 9. Nominal dimensions and material properties of the elementary connections.

Specimen type	Plate type		Screw type
	Steel grade	Thickness [mm]	
SLE	S350GD+Z	1.5	AB 04 63 040
SLD	S350GD+Z	1.5	CI 01 48 016
	S235	2.0	
SHD	S350GD+Z	1.5	AB 04 63 040
	S235	2.0	

Table 10. Test results on elementary connections.

Label	F_t [kN]	k_e [kN/mm]	Failure mode
SLE-01	7.7	2.8	T + PO
SLE-02	7.5	4.6	T + PO
SLE-03	7.6	3.1	T + PO
$exp_{,AV}$	7.7	3.5	-
$exp_{,DEV,ST}$	0.1	1.0	-
$exp_{,COV}$	0.01	0.28	-
th	6.8	-	B
$exp_{,AV} / th$	1.13	-	-
SLD-01	6.5	3.2	S
SLD-02	6.6	3.9	S
SLD-03	6.5	3.0	S
$exp_{,AV}$	6.5	3.4	-
$exp_{,DEV,ST}$	0.1	0.5	-
$exp_{,COV}$	0.01	0.14	-
th	5.2	-	B
$exp_{,AV} / th$	1.26	-	-
SHD-01	9.0	5.7	T + PO
SHD-02	8.9	3.5	T + PO
$exp_{,AV}$	9.0	4.6	-
$exp_{,DEV,ST}$	0.1	1.6	-
$exp_{,COV}$	0.01	0.34	-
th	5.8	-	B
$exp_{,AV} / th$	1.54	-	-

$exp_{,AV}$: average experimental values;
 $exp_{,DEV,ST}$: standard deviation of the experimental values;
 $exp_{,COV}$: coefficient of variation of the experimental values;
th: theoretical values;
T: tilting of screw;
PO: pull-out of screw;
B: bearing failure;
S: shear failure of screw

The results show that the average failure loads of SLE and SHD types are greater than the failure value of SLD specimen, respectively by 17% and 37%. The coefficients of variation show that data have a low scatter distribution, in fact the failure loads have C.O.V. always equal to 1% and the stiffness values have C.O.V. contained between 14% and 34%. The ratios between the average experimental and theoretical values highlight that the experimental strengths are higher of 13%, 26% and 54% for SLE, SLD and SHD specimens, respectively, compared to the theoretical predictions. In addition, the force-displacement curves (Fig. 19a) show a very limited deformation capacity of SLD specimens. The different behaviour is due to dissimilar failure mechanisms: tilting and pull-out of screws for SLE and SHD configurations and shear failure for SLD connections (Fig. 19b).

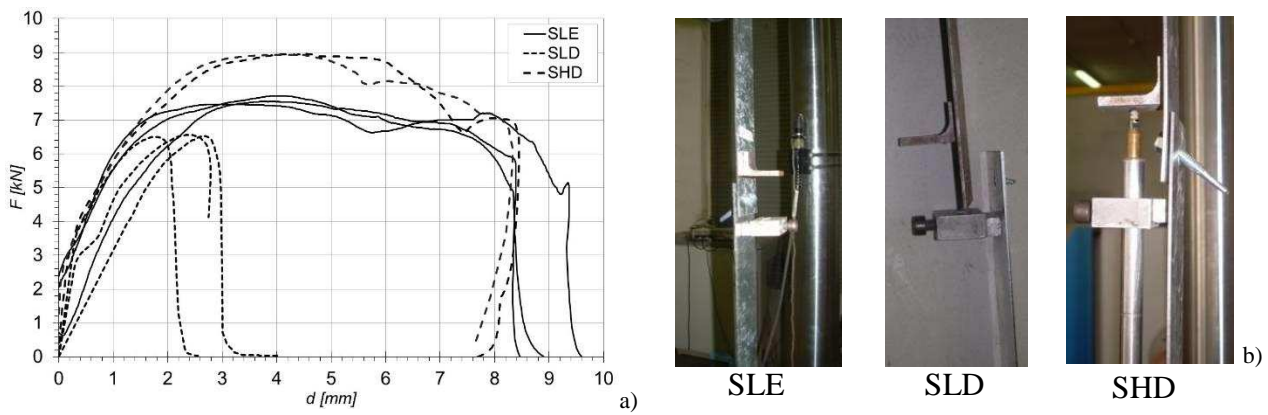


Figure 19. Test on elementary connection: a) F vs. d curves; b) failure modes for SLE, SLD and SHD specimens.

3.3 Tests on frame-to-strap connections

The CFS strap-braced stud walls behaviour is particularly influenced by the design of frame-to-strap connections, which in this case takes place through steel gussets. For this reason, the local response evaluation of the investigated X-braced CFS systems was completed with shear tests on connection prototypes reproducing the joints between gusset and strap-bracing. Table 11 lists the nominal dimensions and material properties of the tested connections. The behaviour of the connections adopted for the three selected wall configurations (indicated with subscript 1) was investigated. Furthermore, three additional connection types for WLD and WHD systems, corresponding to different screw layouts in strap-bracing cross-section, were tested. Therefore, by naming A_{n1} and A_{n2} the minimum net areas defined by considering perpendicular cross-sections to strap-bracing axis and cross-sections obtained by a broken line, respectively, the following joint typologies for dissipative walls were considered (Fig. 20a): (1) connection configuration adopted in the selected walls, in which $A_{n1} < A_{n2}$; (2) connection with aligned screws arrangement; (3) connection with staggered screws, in which $A_{n1} = A_{n2}$; (4) connection with staggered screws, in which $A_{n1} > A_{n2}$. The phenomenon of "strain-rate" was investigated only for the (1) configurations. The experimental values of failure load (F_t) and stiffness (k_c) and the observed failure mechanisms for each test are summarized in Table 12. In addition, Table 12 provides the average experimental values, standard deviation and coefficient of variation (C.O.V.) for strength and stiffness of CLE, CLD and CHD configurations and the ratios between the average experimental and theoretical strength values for only the (1) configurations, which are evaluated according to the EN 1993-1-3 [12] and using the average experimental mechanical properties. The force-displacement curves obtained for the (1) configurations (Fig. 20b) demonstrate that the CHD-1 specimens show the best response in terms of strength and stiffness, with average failure load values approximately twice the values obtained for the CLE-1 and CLD-1 specimens. Furthermore, the strength increases between 5% and 9% and the deformation capacity decreases between 50% and 65% as the test rate increases. As regards the connection response evaluation for different screw geometrical arrangements (Fig. 20c), the configurations do not play significant influence in terms of strength and stiffness, but the (1) connections have larger

deformation capability. The coefficients of variation show that the experimental failure loads are narrowly distributed, with C.O.V. always less than 4%. On the other hand, the stiffness values scattered with C.O.V. up to 25%. The comparison between the average experimental and theoretical values reveals that the experimental strengths recorded at standard rate have maximum differences of 9% compared to the theoretical predictions. For all tests the failure mechanism was screw tilting with subsequent net section failure of straps (Fig. 20d).

The results of tests on elementary and frame-to-strap connection are compared in order to assess the shear stiffness for a single screw. In particular, the average stiffness of a single fastener ranges from 3.4 to 4.6 kN/mm and from 3.8 to 6.0 kN/mm in the tests carried out on elementary connections and on frame-to-strap connections, respectively. Therefore it can be noted that the stiffness values for single screws obtained with frame-to-strap connection tests increases for effect of the group action, with increments of 9%, 18% and 30% for CLE, CLD and CHD compared to SLE, SLD and SHD specimens. The stiffness values of a single screw were considered for the calculation of the wall stiffness due to the deformability of the diagonal-to-frame connections, which is used to evaluate the wall lateral stiffness. More details about this aspect are provided in the companion paper [10].

Table 11. Nominal dimensions and material properties of the frame-to-strap connections.

Specimen type	Plate type		Screw type	No. screws
	Steel grade	Thickness [mm]		
CLE	S350GD+Z	1.5	AB 04 63 040	10
CLD	S350GD+Z	1.5	CI 01 48 016	15
	S235	2.0		
CHD	S350GD+Z	1.5	AB 04 63 040	25
	S235	2.0		

Table 12. Test results on frame-to-strap connections.

Specimen type	Configuration	Label	F_t [kN]		k_c [kN/mm]	k_c/n [kN/mm]	Failure mode
			S	H	S	S	
CLE	CLE-1	CLE-1-01	50.5	55.1	39.4	3.9	T+NSF
		CLE-1-02	50.1	54.8	38.2	3.8	T+NSF
		CLE-1-03	50.5	54.9	36.7	3.7	T+NSF
		CLE_{AV}	50.4	54.9	38.1	3.8	-
		$CLE_{DEV,ST}$	0.2	0.2	1.4	0.1	-
		CLE_{COV}	0.00	0.00	0.04	0.04	-
		th	46.2	46.2	-	-	NSF
		CLE_{AV}/th	1.09	1.19	-	-	-
CLD	CLD-1	CLD-1-01	43.5	48.0	65.0	4.3	T+NSF
		CLD-1-02	43.7	48.0	59.8	4.0	T+NSF
		CLD-1-03	44.3	47.7	51.2	3.4	T+NSF
		exp_{AV}	43.8	47.9	58.7	3.9	-
		th	43.0	43.0	-	-	B
		exp_{AV}/th	1.02	1.11	-	-	-
	CLD-2	CLD-2-01	44.0	-	64.9	4.3	T+NSF

	CLD-2-02	44.4	-	53.3	3.6	T+NSF	
	exp _{,AV}	44.2	-	59.1	3.9	-	
CLD-3	CLD-3-01	44.4	-	46.3	3.1	T+NSF	
	CLD-3-02	44.4	-	66.7	4.4	T+NSF	
	exp _{,AV}	44.4	-	56.5	3.8	-	
	CLD-4-01	43.7	-	53.6	3.6	T+NSF	
CLD-4	CLD-4-02	43.9	-	73.6	4.9	T+NSF	
	exp _{,AV}	43.8	-	63.6	4.2	-	
	CLD _{,AV}	44.0	47.9	59.4	4.0	-	
	CLD _{,DEV.ST}	0.4	0.2	8.8	0.6	-	
	CLD _{,COV}	0.01	0.00	0.15	0.15	-	
CHD	CHD-1-01	91.0	95.1	155.6	6.2	T+NSF	
	CHD-1-02	90.5	-	161.7	6.5	T+NSF	
	CHD-1	CHD-1-03	89.4	-	181.8	7.3	T+NSF
		exp _{,AV}	90.3	95.1	166.4	6.7	-
		th	87.0	87.0	-	-	NSF
		exp _{,AV} / th	1.04	1.09	-	-	-
	CHD-2	CHD-2-01	85.3	-	94.9	3.8	T+NSF
		CHD-2-02	83.6	-	143.3	5.7	T+NSF
		exp _{,AV}	84.5	-	119.1	4.8	-
	CHD-3	CHD-3-01	83.1	-	129.8	5.2	T+NSF
		CHD-3-02	86.6	-	97.6	3.9	T+NSF
		exp _{,AV}	84.9	-	113.7	4.5	-
	CHD-4	CHD-4-01	84.0	-	211.5	8.5	T+NSF
		CHD-4-02	84.8	-	170.0	6.8	T+NSF
		exp _{,AV}	84.4	-	190.8	7.6	-
		CHD _{,AV}	86.5	95.1	149.6	6.0	-
		CHD _{,DEV.ST}	3.1	-	38.1	1.5	-
		CHD _{,COV}	0.04	-	0.25	0.25%	-

AV : average experimental values;
 DEV.ST: standard deviation of the experimental values;
 COV: coefficient of variation of the experimental values;
 th: theoretical values;
 n: number of screws;
 T: tilting of screw;
 NSF: net section failure of strap-bracing;
 B: bearing failure;
 H: high rate (50 mm/s);
 S: standard rate (0.05 mm/s)

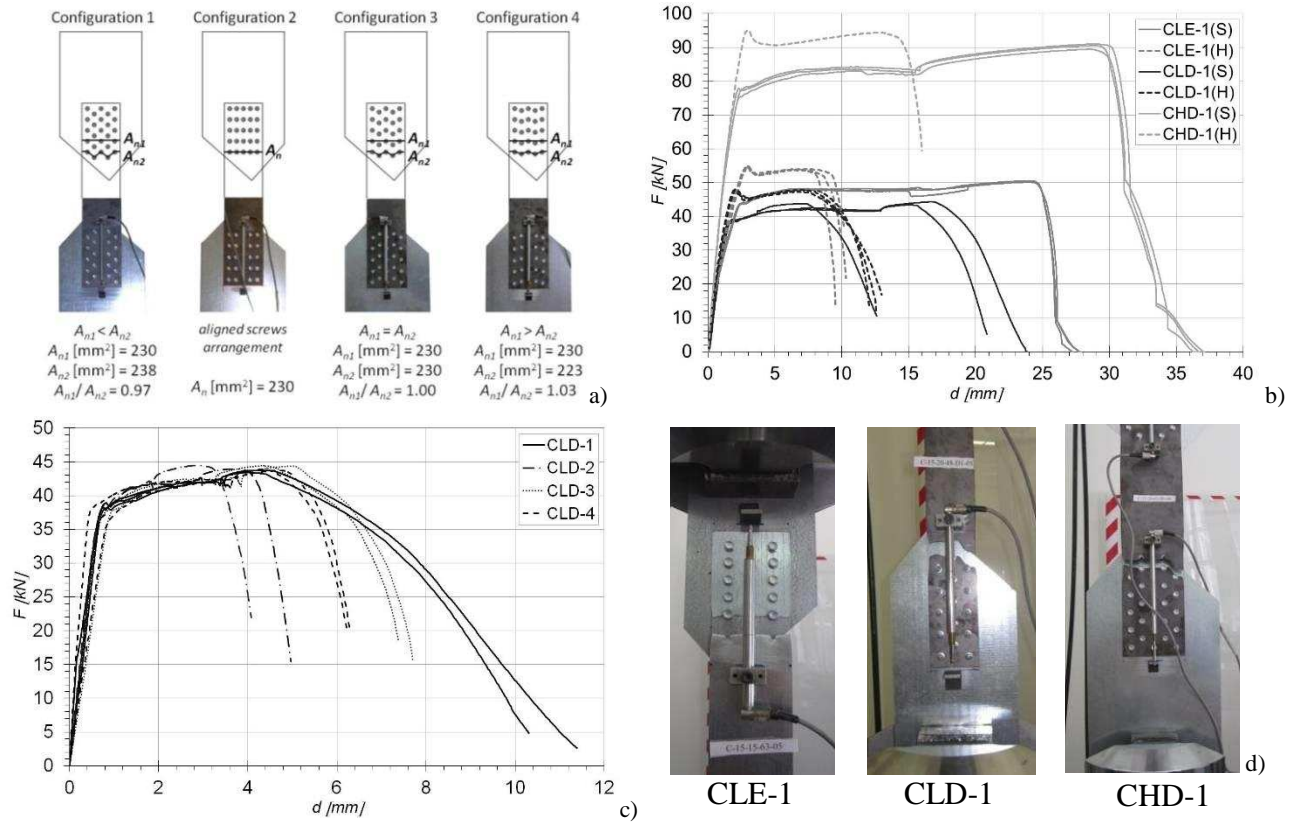


Figure 20. Test on frame-to-strap connections: a) CHD specimens; b) F vs. d curves for type 1 configurations; c) F vs. d curves for CLD specimens; d) failure modes for CLE-1, CLD-1 and CHD-1 specimens.

4 EXPERIMENTAL VALIDATION OF THE DESIGN CRITERIA

In order to validate the design criteria for the investigated seismic resistant system, the prescriptions and requirements provided by EN 1998-1 [9] and AISI S213 [19] have been also evaluated on the basis of the results obtained in the experimental campaign, in which full-scale and component tests have been carried out.

For each selected wall configuration, a preliminary evaluation of the behaviour factor based on the results of monotonic and cyclic wall tests has been carried out (Fig. 21). The behaviour factor has been defined by the ductility-related (R_d) and overstrength-related (R_o) modification factors, as given in Uang [21]:

$$q = R_d \cdot R_o \quad (4)$$

Considering that the fundamental periods for this structural typology is generally ranging between 0.1 and 0.5 s, the ductility-related force modification factor R_d can be evaluated as follows:

$$R_d = \sqrt{2\mu - 1} \quad \text{with} \quad \mu = \frac{d_{\max}}{d_y} \quad (5)$$

where μ is the ductility; d_{\max} e d_y are the maximum and the conventional elastic limit of the top wall displacement, respectively. The displacement d_{\max} has been defined as the displacement corresponding to the following limits of interstorey-drift (d/h , with $h=2700$ mm as wall height): 1.5%, 2% and 7%. For the cases in which the wall collapse occurred for displacement lower than the given limits, d_{\max} has been assumed as the displacement at the peak load. The limits of 1.5% and 2% are those provided by FEMA 356 [13] for traditional concentrically braced structures at the Life Safety and Collapse Prevention limit states, respectively. On the other hand, the limit of 7% is the maximum displacement capacity obtained by shaking table tests [22] on wooden shear walls, which represent a system similar to the investigated one.

The overstrength-related force modification factor R_o can be evaluated through the formulation provided by Mitchell et al. [23]:

$$R_o = R_{sd} \cdot R_{\phi} \cdot R_{yield} \cdot R_{sh} \quad (6)$$

where $R_{sd} = H_c/H_d$, with H_c and H_d design wall resistance and seismic demand, respectively; $R_{\phi} = H_{yn}/H_c$, with H_{yn} nominal yielding resistance; $R_{yield} = H_y/H_{yn}$, with H_y experimental yielding resistance (average); $R_{sh} = H_{\%}/H_y$, with $H_{\%}$ wall resistance at relevant inter-story drift.

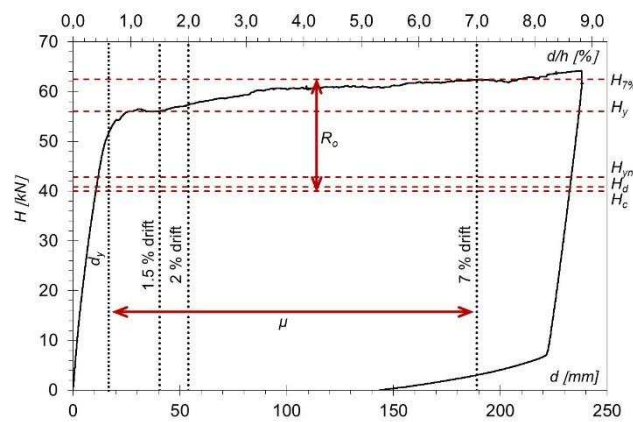


Figure 21. Tests-based behaviour factor evaluation

Tables 13 and 14 show the values of the behaviour factor obtained by the experimental results. In particular, for WLE walls d_{\max}/h result always less than 1.5%, so the evaluation of q is limited to the case $d=d_{\max}$. In the case of WLE walls (Table 13), it can be noted that the behaviour factor values proposed by AISI S213 for Conventional construction category ($q=1.6$) is always smaller than those experimentally obtained ($q=2.0\div 2.2$). In particular, the obtained values of overstrength factor are very uniform ($R_o=1.2$) and slightly lower than the one provided by code ($R_o=1.3$). On the contrary, the measured ductility factors ($R_d=1.7\div 1.8$) are always greater than the provided value ($R_d=1.2$).

As far as WLD and WHD walls are concerned, the value provided by AISI S213 in case of Limited ductility braced walls ($q=2.5$) represents a lower limit of the obtained behaviour factors ($q=2.5\div 3.0$).

for 1.5%, $q=3.0\div 4.3$ for 2%, $q=6.4\div 8.2$ for 7%) (Table 14). In this case, it can be noticed that the obtained values of both overstrength ($R_o=1.4\div 1.6$) and ductility factor ($R_d=1.9\div 5.3$) are greater than AISI S213 values ($R_o=1.3$ and $R_d=1.9$), with the only exception of WHD-M2 case ($R_d=1.8$) for 1.5% drift limit.

As it is well known, the methodology used to evaluate the behaviour factor does not explicitly take into account of the load-deformation hysteresis "shape", which for the examined structural typology is characterized by a relevant pinching. Therefore, the obtained results in terms of q-values should be validated using more advanced methods, such as non-linear time history dynamic analysis.

Table 13. Behaviour factor for WLE.

Test	R_d	R_o	q
WLE-M1	1.74	1.15	2.00
WLE-M2	1.74	1.17	2.04
WLE-C1	1.80	1.21	2.19
WLE-C2	1.73	1.20	2.08

Table 14. Behaviour factor for WLD and WHD.

Test	1.5% interstorey drift			2% interstorey drift			7% interstorey drift		
	R_d	R_o	q	R_d	R_o	q	R_d	R_o	q
WLD-M1	2.18	1.42	3.09	2.58	1.43	3.68	5.08	1.53	7.76
WLD-M2	2.28	1.40	3.20	2.70	1.43	3.87	5.29	1.56	8.24
WLD-C1	2.18	1.51	3.29	2.58	1.50	3.88	5.08	1.53	7.75
WLD-C2	2.39	1.53	3.65	2.82	1.51	4.26	4.77	1.64	7.83
WHD-M1	1.89	1.38	2.60	2.26	1.38	3.11	(*)		
WHD-M2	1.83	1.37	2.51	2.19	1.41	3.08	4.40	1.46	6.40
WHD-C1	1.96	1.45	2.84	2.33	1.46	3.41	4.64	1.51	7.02
WHD-C2 (Pull)	2.12	1.41	2.99	2.52	1.44	3.63	(**)		
WHD-C2 (Push)	1.98	1.41	2.80	2.36	1.44	3.39	4.69	1.41	6.64

(*) The test was interrupted because of the occurrence of local buckling of the tracks;

(**) The diagonal net area collapse before reaching the limit of 7%.

It has to be noticed that the experimental evidence showed that the design formulation (Eq. 1 in Tab. 1), aimed at preventing the failure of the diagonal net area at fastener holes, is not always effective. In fact, even if the diagonal connections of dissipative configurations (WLD and WHD) were designed according to Eq. 1, the failure mechanism observed in all connection tests and cyclic wall tests always corresponds to the net area fracture, as illustrated in Sections 2.2 and 3.3. In fact, for the dissipative walls, only in the case of monotonic tests the yielding of the tension diagonals was reached without ruptures in the field of the investigated displacements (drift higher than 5.1%), while for the cyclic tests the response was always affected by net area failure (drift higher than 2.5%). However, the obtained drift levels are always larger than ones which typically be occurred in an actual structures

during a design level earthquake and they are greater than the drift limits of 1.5% and 2% provided in FEMA 356 [13] for traditional concentrically braced structures.

The different failure mechanisms observed for connections and monotonic wall tests can be explained by comparing the strain levels reached in the two cases. In Figure 22, the experimental curves in terms of axial force vs. strain in the flat strap for connection and monotonic wall tests are depicted together with the experimental stress-strain curves of steel material. In particular, the strain in connection and wall tests were measured on a base length of 250 and 2750 mm, respectively. It can be observed that the strain levels at ultimate condition in the case of connections (ε_c) are significantly higher than those obtained in wall tests (ε_w). The corresponding stress level (σ_c) for connections is close to the ultimate strength of the material while, in the wall tests, the stress (σ_w) is on yield plateau. Therefore, the connection behaviour at failure is conditioned by high strain levels and the hardening implies the failure of the net section. On the contrary, in the case of walls, due to the lower strain levels the maximum force in the diagonal gross section is not enough to entail the failure of the net area. As a conclusion, it seems that the Eq. 1 is reliable only for low strain levels. For the sake of clarity, it is relevant to notice that in this comparisons the effect of corner restraint provided by the gusset plates in the wall has been neglected. Therefore, the actual stress distribution in the strap could be affected by this effect. As a result, the stress distribution in the connection tests could be a more ideal (uniform) tension loading condition compared with that in the strap.

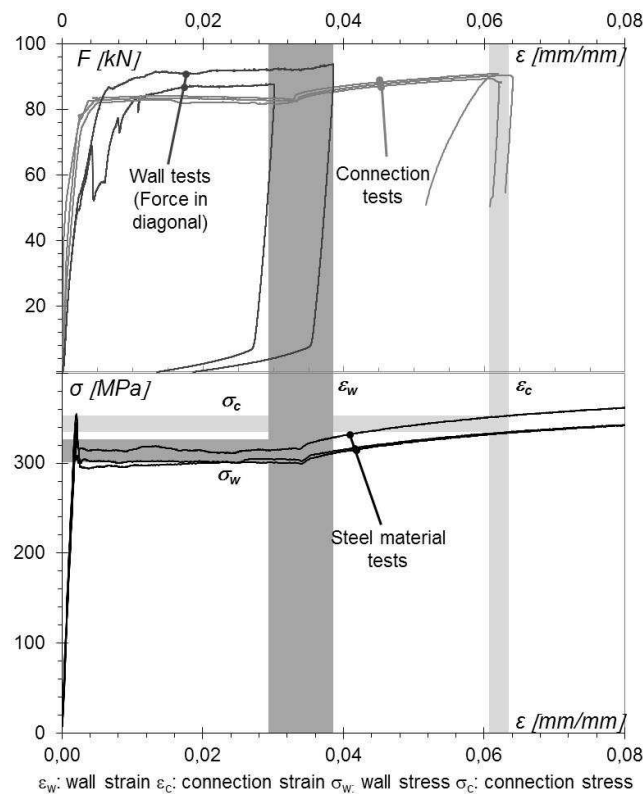


Figure 22. Comparison of deformation related to testing of diagonal strap-braced walls and connection

As far as the ultimate behaviour in the hysteretic field is concerned, the occurrence of net sections failures observed in the cyclic wall tests, can be caused by low cycle fatigue phenomena amplified by the stress concentrations at the fastener holes.

As far as the capacity design criteria are concerned, the experimental results showed that the adopted formulation (Eq. 2 in Tab. 1) is able to preserve the seismic-resistant system from undesirable brittle failures of connections, tracks, studs and anchorages. Similar considerations can be also made for the formulation used to provide an adequate deformation capacity to the connections (Eq. 3 in Tab. 1). In fact, no shear failure of the screws occurred in both connections and wall tests. The experimental results do not allow to make any consideration about the global mechanism because the tests performed on walls are representative of only one storey.

CONCLUSIONS

This paper presents and discusses an experimental investigation carried out for the evaluation of the seismic behaviour of CFS strap-braced constructions. The experimental campaign aimed to study the global inelastic response of a wide range of X-braced walls, designed according to both an elastic and dissipative approach. Moreover, the local behaviour was investigated by tests on material and the main connection systems. The results showed a satisfactory response between predicted and experimental behaviour of walls and connection systems in terms of strength, deformation capacity and stiffness. In particular, a good correspondence between wall experimental and theoretical predicted values was highlighted in terms of strength (maximum gap of 14%). The experimental study also highlighted that the wall corners should be carefully designed and executed, since their behaviour may significantly affect the overall wall response. Furthermore, the experimental results allowed the validation of assumed design hypotheses. The behaviour factor values provided by AISI S213 are widely confirmed by the experimental tests and, the code values represents lower limits of the one obtained experimentally. In addition, the requirements concerning the capacity design given in the Eurocodes, for traditional systems, are also reliable for the CFS structures.

These experimental results have been considered as reference for theoretical studies aimed at defining seismic design criteria for the investigated systems. As a further development, an extended numerical study including non-linear dynamic analysis should be performed for a more accurate estimation of the behaviour factor. These analysis should be carried out on case studies representative of single and multi-storey buildings. In addition, shaking table tests on 3D structures and tests on prototypes representative of multi-storey buildings should be carried out, in order to obtain a complete overview of the seismic performance of the investigated structural typology.

ACKNOWLEDGMENT

The authors acknowledge the Department of Civil Protection for the financial support to the research activity and the following companies: Guerrasio S.r.L. for the furnishing of steel profiles, TECFI S.p.A. for the screws and KNAUF for the collaboration to the specimens assembling. The authors would also like to thank the anonymous reviewer for the precious comments and suggestions to improve the quality of the paper.

REFERENCES

- [1] Fiorino, L., Della Corte, G., Landolfo, R., 2005. Seismic response of light-gauge steel stick-built constructions: summary of a research project. In Proceedings of the COST C12 Final Conference - Improving buildings' structural quality by new technologies. Innsbruck, Austria. Schaur et al. (eds.). Taylor & Francis Group Publisher. pp. 105-113.
- [2] Landolfo, R., Fiorino, L., Della Corte, G., 2006. Seismic behavior of sheathed cold-formed structures: physical tests. *Journal of Structural Engineering*. ASCE. Vol. 132, No. 4, pp. 570-581.
- [3] Landolfo, R., Della Corte, G., Fiorino, L., 2006. Shear behavior of connections between cold-formed steel profiles and wood or gypsum - based panels: an experimental investigation. In Proceedings of the 2006 Structures Congress. St. Louis, Missouri, USA. Published by the American Society of Civil Engineers. On CD-ROM.
- [4] Fiorino, L., Della Corte, G., Landolfo, R., 2006. Experimental tests on sheathing-to-stud screw connections. In Proceedings of the Progress in Steel, Composite and Aluminium Structures (ICMS 2006). Rzeszów, Poland. Giżejowski, Kozłowski, Ślęczka & Ziółko (eds). Taylor & Francis Group Publisher. pp. 409-417. On CD-ROM.
- [5] Fiorino, L., Della Corte, G., Landolfo, R., 2007. Experimental tests on typical screw connections for cold-formed steel housing. *Engineering Structures*. Elsevier Science. Vol. 29, pp. 1761–1773.
- [6] Iuorio, O., 2007. Cold-formed steel housing. *POLLACK PERIODICA*. An International Journal for Engineering and Information Sciences. December 2007, vol. 2-3, pp. 97-108.
- [7] Fiorino, L., Landolfo, R., Iuorio, O., 2008. Experimental response of connections between cold-formed steel profile and cement-based panel. In Proceedings of the 19th International Specialty Conference on Cold-formed Steel Structures. St. Louis, MO, USA. pp. 603-619.
- [8] Iuorio O., Fiorino L., Landolfo R., 2014 Testing CFS Structures: The New School BFS Naples. *Thin-Walled Structures*, Elsevier Science, vol. 84 pp. 275–288.
- [9] CEN, EN 1998-1-1, Eurocode 8, Design of structures for earthquake resistance - Part 1-1: General rules, seismic actions and rules for buildings. European Committee for Standardization, Bruxelles, 2005.
- [10] Macillo, V., Iuorio, O., Terracciano, M.T., Fiorino, L., Landolfo, R., in publication. Seismic response of CFS strap-braced stud walls: Theoretical study. *Thin-Walled Structures*, under review.
- [11] Tecfi, 2014. General Catalogue n°4 exp. Tecfi S.p.A.

- [12] CEN, EN 1993-1-3, Eurocode 3, Design of steel structures - Part 1-3: General rules – Supplementary rules for cold-formed members and sheeting, European Committee for Standardization, Bruxelles, 2006.
- [13] FEMA 356, Prestandard and Commentary for the Seismic Rehabilitation of Buildings, American Society of Civil Engineers, Washington, DC, 2000.
- [14] Krawinkler, H., Parisi, F., Ibarra, L., Ayoub, A., Medina, R., 2000. Development of a testing protocol for woodframe structures. Report W-02, CUREE/Caltech woodframe project. Richmond (CA, USA).
- [15] Velchev, K., Comeau, G., Balh, N., Rogers, C.A., 2010. Evaluation of the AISI S213 seismic design procedures through testing of strap braced cold-formed steel walls. *Thin-Walled Structures*, Vol. 48, pp. 846-856.
- [16] UNI EN ISO 6892-1: 2009. Metallic materials - Tensile testing - Part 1: Method of test at room temperature. European committee for standardization.
- [17] Velchev, K., Rogers, C.A., “Inelastic Performance of Screw Connected Strap Braced Walls” M.Eng. Thesis, Department of Civil Engineering and Applied Mechanics, McGill University, Montreal, Quebec, Canada, 2008.
- [18] Serrette, R.L. "Additional Shear Wall Values for Light Weight Steel Framing" Final Report, Santa Clara University, Santa Clara, CA, 1997.
- [19] AISI, AISI S213-07/S1-09 North American Standard for Cold-Formed Steel Framing – Lateral Design 2007 Edition with Supplement No. 1, American Iron and Steel Institute (AISI), Washington, DC, 2009.
- [20] ECCS TC7 TWG 7.10: 2009. The testing of connections with Mechanical Fasteners in Steel Sheeting and Sections. European Convention for Constructional Steelwork.
- [21] Uang, C.M., 1991. Establishing R (or R_w) and Cd Factors for Building Seismic Provisions. *Journal of structural Engineering*, Vol. 117.
- [22] Isoda, H., Furuya, O., Tatsuya, M., Hirano, S. and Minowa, C., 2007. Collapse behavior of wood house designed by minimum requirement in law. *Journal of Japan Association for Earthquake Engineering*.
- [23] Mitchell, D., Tremblay, R., Karacabeyli, E., Paulte, P., Saatcioglu, M., Anderson, D.L., 2003. Seismic Force Modification Factors for the Proposed 2005 Edition of the National Building Code of Canada. *Canadian Journal of Civil Engineering* 30(2), pp. 308-327.